

A Proximal Variable Smoothing for Nonsmooth Minimization Involving Weakly Convex Composite with MIMO Application

Keita Kume*, Isao Yamada†

Dept. of Information and Communications Engineering, Tokyo Institute of Technology

Email: *kume@sp.ce.titech.ac.jp, †isao@sp.ce.titech.ac.jp

Abstract—We propose a proximal variable smoothing algorithm for nonsmooth optimization problem with sum of three functions involving weakly convex composite function. The proposed algorithm is designed as a time-varying forward-backward splitting algorithm with two steps: (i) a time-varying forward step with the gradient of a smoothed surrogate function, designed with the Moreau envelope, of the sum of two functions; (ii) the backward step with a proximity operator of the remaining function. For the proposed algorithm, we present a convergence analysis in terms of a stationary point by using a newly smoothed surrogate stationarity measure. As an application of the target problem, we also present a formulation of multiple-input-multiple-output (MIMO) signal detection with phase-shift keying. Numerical experiments demonstrate the efficacy of the proposed formulation and algorithm.

Index Terms—nonsmooth optimization, weakly convex composite, Moreau envelope, variable smoothing, MIMO signal detection

I. INTRODUCTION

In this paper, we address the following (possibly nonsmooth and nonconvex) optimization problem with sum of three functions:

Problem I.1. Let \mathcal{X} and \mathcal{Z} be Euclidean spaces, i.e., finite-dimensional real Hilbert spaces. Then,

$$\text{find } \mathbf{x}^* \in \underset{\mathbf{x} \in \mathcal{X}}{\text{argmin}} (h + g \circ \mathfrak{S} + \phi)(\mathbf{x}) (= (f + \phi)(\mathbf{x})),$$

where ϕ , h , \mathfrak{S} , g , and $f := h + g \circ \mathfrak{S}$ satisfy the following:

- (i) $\phi : \mathcal{X} \rightarrow \mathbb{R} \cup \{+\infty\}$ is a proper lower semicontinuous convex function, and *prox-friendly*, i.e., the proximity operator $\text{prox}_{\gamma\phi}$ ($\gamma \in \mathbb{R}_{++}$) (see (3)) is available as a computational tool (such a ϕ includes, e.g., the projection onto a nonempty (simple) closed convex set);
- (ii) $h : \mathcal{X} \rightarrow \mathbb{R}$ is differentiable and its gradient $\nabla h : \mathcal{X} \rightarrow \mathcal{X}$ is Lipschitz continuous over $\text{dom}(\phi) := \{\mathbf{x} \in \mathcal{X} \mid \phi(\mathbf{x}) < +\infty\}$;
- (iii) $\mathfrak{S} : \mathcal{X} \rightarrow \mathcal{Z}$ is a continuously differentiable mapping;
- (iv) $g : \mathcal{Z} \rightarrow \mathbb{R}$ is (a) Lipschitz continuous (possibly nonsmooth), (b) η -weakly convex with $\eta > 0$, i.e., $g + \frac{\eta}{2} \|\cdot\|^2$ is convex, and (c) prox-friendly (such a g includes, e.g., ℓ_1 -norm $\|\cdot\|_1$ [1], minimax concave penalty (MCP) [2], and smoothly clipped absolute deviation (SCAD) [3]);
- (v) $\inf\{(f + \phi)(\mathbf{x}) \mid \mathbf{x} \in \text{dom}(\phi)\} > -\infty$.

Problem I.1 has attracted tremendous attentions because of its potential for flexible formulation to align with many signal processing and machine learning applications (see, e.g., a recent review paper [4]). Indeed, in a special case where \mathfrak{S} is linear, such applications include, e.g., tensor completion [5], principal component pursuit [6], and block sparse recovery [7], to name a few (see, e.g., [8]). In more general cases where \mathfrak{S} is nonlinear but smooth, Problem I.1 is also known to have a wide range of applications, e.g., robust phase retrieval [9], robust matrix recovery [10], and robust blind deconvolution [11], to name a few (see, e.g., [12], [13]).

For Problem I.1 with some special cases, proximal splitting-type algorithms have been used. For example, in a convex case where h , g ,

and ϕ are convex and \mathfrak{S} is linear, Davis-Yin's three-operator splitting algorithm [14], [15] has been designed with the gradient of h and the proximity operators of g and ϕ . In particular with $g = 0$, we can use the forward-backward splitting algorithm (also known as the proximal gradient method), e.g., [1], [16], which consists of (i) the forward step with the gradient ∇h and (ii) the backward step with $\text{prox}_{\gamma\phi}$ ($\gamma > 0$). For general Problem I.1, the so-called prox-linear method [12], [13] is designed with a solution to a certain proximal subproblem that is a minimization of a linearized function of $g \circ \mathfrak{S}$. Although the prox-linear method is guaranteed to converge to a stationary point in the sense of zero of the general subdifferential (see (1)), the prox-linear method requires some iterative solver for the proximal subproblem at every iteration.

Inspired by [17]–[19], in this paper, we propose for Problem I.1 a proximal variable smoothing which does not require any iterative solver at each iteration. Indeed, the proposed algorithm in Alg. 1 is designed as a time-varying forward-backward splitting-type (or proximal gradient-type) algorithm designed with the Moreau envelope ${}^\mu g$ ($\mu \in (0, \eta^{-1})$) of g (see (4)). More precisely, the proposed algorithm consists of two steps: (i) the forward step with the gradient of a time-varying smoothed surrogate function $f_n := h + {}^\mu g \circ \mathfrak{S}$ ($\mu_n \in (0, \eta^{-1}) \searrow 0$) of $f = h + g \circ \mathfrak{S}$ and (ii) the backward step with $\text{prox}_{\gamma_n\phi}$ (see (3)) with a stepsize $\gamma_n > 0$.

We also present an asymptotic convergence analysis, in Theorem III.4, of the proposed algorithm in terms of a stationary point. The proposed convergence analysis relies on a smooth approximation of a stationarity measure $\mathcal{M}_{\gamma}^{f,\phi}$ ($\gamma > 0$) [19] in (5) with the smoothed surrogate function f_n (see also Theorem III.1).

The proposed algorithm and analysis serve as an extension of variable smoothing-type algorithms [17]–[19] because Problem I.1 covers the cases assumed in [17]–[19] (see Remark III.5). For example, convex constrained minimizations of the composition of a (weakly) convex function and a smooth function have been key models in signal processing (see, e.g., [10]–[13]). However, the existing algorithms [17]–[19] cannot be applied to such cases, while the proposed algorithm can be applied.

To verify the effectiveness of the proposed algorithm, we present numerical experiments in a scenario of MIMO signal detection [20]–[23] with its new formulation via Problem I.1 (see Section IV).

Notation: \mathbb{N} , \mathbb{Z} , \mathbb{R} , \mathbb{R}_{++} , and \mathbb{C} denote respectively the sets of all positive integers, all integers, all real numbers, all positive real numbers, and all complex numbers (i stands for the imaginary unit, and \Re and \Im stand respectively for real and imaginary parts). The symbol $\mathbf{1}$ is the vector of all ones. For a given matrix $\mathbf{A} \in \mathbb{K}^{L \times M}$ and a vector $\mathbf{v} \in \mathbb{K}^N$ ($\mathbb{K} = \mathbb{R}, \mathbb{C}$), $[\mathbf{A}]_{l,m} \in \mathbb{K}$ and $[\mathbf{v}]_n \in \mathbb{K}$ denote respectively the (l, m) entry of \mathbf{A} and n th entry of \mathbf{v} . The symbol \odot is the element-wise product, i.e., $[\mathbf{a} \odot \mathbf{b}]_n := [\mathbf{a}]_n [\mathbf{b}]_n$ ($\mathbf{a}, \mathbf{b} \in \mathbb{R}^N$), $\|\cdot\|$ and $\langle \cdot, \cdot \rangle$ are respectively the Euclidean norm and the standard inner product. For a linear operator $A : \mathcal{X} \rightarrow \mathcal{Z}$, $\|A\|_{\text{op}} := \sup_{\|\mathbf{x}\| \leq 1, \mathbf{x} \in \mathcal{X}} \|A\mathbf{x}\|$ denotes the operator norm of A .

For a continuously differentiable mapping $\mathcal{F} : \mathcal{X} \rightarrow \mathcal{Z}$, its Gâteaux derivative at $\mathbf{x} \in \mathcal{X}$ is the linear operator $D\mathcal{F}(\mathbf{x}) : \mathcal{X} \rightarrow \mathcal{Z} : \mathbf{v} \mapsto \lim_{\mathbb{R} \setminus \{0\} \ni t \rightarrow 0} \frac{\mathcal{F}(\mathbf{x}+t\mathbf{v}) - \mathcal{F}(\mathbf{x})}{t}$. For a Gâteaux differentiable function $J : \mathcal{X} \rightarrow \mathbb{R}$, $\nabla J(\mathbf{x}) \in \mathcal{X}$ is the gradient of J at $\mathbf{x} \in \mathcal{X}$ if $DJ(\mathbf{x})[\mathbf{v}] = \langle \nabla J(\mathbf{x}), \mathbf{v} \rangle$ ($\mathbf{v} \in \mathcal{X}$). For a function $J : \mathcal{X} \rightarrow \mathbb{R} \cup \{+\infty\}$, J is called (a) proper if $\text{dom}(J) := \{\mathbf{x} \in \mathcal{X} \mid J(\mathbf{x}) < +\infty\} \neq \emptyset$; (b) lower semicontinuous if $\{(\mathbf{x}, a) \in \mathcal{X} \times \mathbb{R} \mid J(\mathbf{x}) \leq a\} \subset \mathcal{X} \times \mathbb{R}$ is closed in $\mathcal{X} \times \mathbb{R}$, or equivalently, $\liminf_{n \rightarrow \infty} J(\mathbf{x}_n) \geq J(\bar{\mathbf{x}})$ for every $\bar{\mathbf{x}} \in \mathcal{X}$ and every $(\mathbf{x}_n)_{n=1}^{\infty} \subset \mathcal{X}$ converging to $\bar{\mathbf{x}}$; (c) convex if $J(t\mathbf{x}_1 + (1-t)\mathbf{x}_2) \leq tJ(\mathbf{x}_1) + (1-t)J(\mathbf{x}_2)$ ($\forall t \in [0, 1], \forall \mathbf{x}_1, \mathbf{x}_2 \in \mathcal{X}$).

II. PRELIMINARY ON NONSMOOTH ANALYSIS

We review some necessary notions in nonsmooth analysis primarily based on notations in [1], [24] (see also a review paper [4]).

Definition II.1 (Subdifferential [24, Def. 8.3]). For a possibly nonconvex function $J : \mathcal{X} \rightarrow \mathbb{R} \cup \{+\infty\}$, the general subdifferential $\partial J : \mathcal{X} \rightrightarrows \mathcal{X}$ of J at $\bar{\mathbf{x}} \in \text{dom}(J)$ is defined by

$$\partial J(\bar{\mathbf{x}}) := \left\{ \mathbf{v} \in \mathcal{X} \mid \bar{\mathbf{x}} = \lim_{n \rightarrow \infty} \mathbf{x}_n, J(\bar{\mathbf{x}}) = \lim_{n \rightarrow \infty} J(\mathbf{x}_n), \mathbf{v} = \lim_{n \rightarrow \infty} \mathbf{v}_n \right\}, \quad (1)$$

where^{a)} $\hat{\partial}J(\bar{\mathbf{x}}) := \left\{ \mathbf{v} \in \mathcal{X} \mid \liminf_{\substack{\mathcal{X} \ni \mathbf{x} \rightarrow \bar{\mathbf{x}} \\ \mathbf{x} \neq \bar{\mathbf{x}}}} \frac{J(\mathbf{x}) - J(\bar{\mathbf{x}}) - \langle \mathbf{v}, \mathbf{x} - \bar{\mathbf{x}} \rangle}{\|\mathbf{x} - \bar{\mathbf{x}}\|} \geq 0 \right\}$ is called the regular subdifferential of J at $\bar{\mathbf{x}} \in \text{dom}(J)$, where $\partial J(\bar{\mathbf{x}})$ and $\hat{\partial}J(\bar{\mathbf{x}})$ at $\bar{\mathbf{x}} \notin \text{dom}(J)$ are understood as \emptyset . If J is convex, then ∂J and $\hat{\partial}J$ coincide with the convex subdifferential of J .

By Fermat's rule [24, Theorem 10.1], a local minimizer $\mathbf{x}^* \in \mathcal{X}$ of $f + \phi$ in Problem I.1 satisfies the first-order optimality condition:

$$\partial(f + \phi)(\mathbf{x}^*) = \partial f(\mathbf{x}^*) + \partial\phi(\mathbf{x}^*) \ni \mathbf{0}, \quad (2)$$

where the equality can be checked by [24, Corollary 10.9]. We call \mathbf{x}^* satisfying (2) stationary point of $f + \phi$, and we focus on finding a stationary point of $f + \phi$ throughout this paper.

The proximity operator and the Moreau envelope have been used as computational tools for nonsmooth optimization [1], [25]–[27]. For an $\eta (> 0)$ -weakly convex function g , its proximity operator and Moreau envelope of index $\mu \in (0, \eta^{-1})$ are respectively defined by

$$(\bar{\mathbf{z}} \in \mathcal{Z}) \quad \text{prox}_{\mu g}(\bar{\mathbf{z}}) := \underset{\mathbf{z} \in \mathcal{Z}}{\text{argmin}} \left(g(\mathbf{z}) + \frac{1}{2\mu} \|\mathbf{z} - \bar{\mathbf{z}}\|^2 \right); \quad (3)$$

$$(\bar{\mathbf{z}} \in \mathcal{Z}) \quad \mu g(\bar{\mathbf{z}}) := \min_{\mathbf{z} \in \mathcal{Z}} \left(g(\mathbf{z}) + \frac{1}{2\mu} \|\mathbf{z} - \bar{\mathbf{z}}\|^2 \right), \quad (4)$$

where $\text{prox}_{\mu g}$ is single-valued due to the strong convexity of $g + (2\mu)^{-1} \|\cdot - \bar{\mathbf{z}}\|^2$. Many functions g have the close-form expressions of $\text{prox}_{\mu g}$ and μg , e.g., ℓ_1 -norm, MCP, and SCAD (see, e.g., [28]). The Moreau envelope μg serves as a smoothed surrogate function of g because $\lim_{\mu \rightarrow 0} \mu g(\mathbf{z}) = g(\mathbf{z})$ ($\mathbf{z} \in \mathcal{Z}$), and μg is continuously differentiable with $\nabla \mu g(\mathbf{z}) = \mu^{-1}(\mathbf{z} - \text{prox}_{\mu g}(\mathbf{z}))$ (see, e.g., [27]). Moreover, $\nabla \mu g$ is Lipschitz continuous [29, Corollary 3.4].

III. PROXIMAL VARIABLE SMOOTHING

We employ the following stationarity measure [19] at a given $\bar{\mathbf{x}} \in \mathcal{X}$ with $\gamma \in \mathbb{R}_{++}$ in order to measure an achievement level of the first-order optimality condition in (2):

$$\mathcal{M}_{\gamma}^{f, \phi}(\bar{\mathbf{x}}) := \inf \left\{ \gamma^{-1} \|\bar{\mathbf{x}} - \text{prox}_{\gamma\phi}(\bar{\mathbf{x}} - \gamma\mathbf{v})\| \mid \mathbf{v} \in \partial f(\bar{\mathbf{x}}) \right\}. \quad (5)$$

^{a)}The limit inferior [24, Definition 1.5] is given by

$$\liminf_{\substack{\mathcal{X} \ni \mathbf{x} \rightarrow \bar{\mathbf{x}} \\ \mathbf{x} \neq \bar{\mathbf{x}}}} \frac{J(\mathbf{x}) - J(\bar{\mathbf{x}}) - \langle \mathbf{v}, \mathbf{x} - \bar{\mathbf{x}} \rangle}{\|\mathbf{x} - \bar{\mathbf{x}}\|} = \sup_{\epsilon > 0} \left(\inf_{0 < \|\mathbf{x} - \bar{\mathbf{x}}\| < \epsilon} \frac{J(\mathbf{x}) - J(\bar{\mathbf{x}}) - \langle \mathbf{v}, \mathbf{x} - \bar{\mathbf{x}} \rangle}{\|\mathbf{x} - \bar{\mathbf{x}}\|} \right).$$

Algorithm 1 Proximal variable smoothing for Problem I.1

Require: $\mathbf{x}_1 \in \mathcal{X}, c \in (0, 1), (\mu_n)_{n=1}^{\infty} \subset (0, (2\eta)^{-1}]$ satisfying (6)
for $n = 1, 2, \dots$ **do**
 Set $f_n := h + \mu_n g \circ \mathfrak{S}$
 Find $\gamma_n > 0$ satisfying Assumption III.2 (b) (see Remark III.3 (b))
 $\mathbf{x}_{n+1} \leftarrow \text{prox}_{\gamma_n \phi}(\mathbf{x}_n - \gamma_n \nabla f_n(\mathbf{x}_n))$
end for
Ensure: $\mathbf{x}_n \in \mathcal{X}$

The measure $\mathcal{M}_{\gamma}^{f, \phi}$ serves as a generalization of commonly-used stationarity measures. Indeed, with a special case $\phi \equiv 0$, $\mathcal{M}_{\gamma}^{f, \phi}(\bar{\mathbf{x}}) = d(\mathbf{0}, \partial f(\bar{\mathbf{x}}))$ ($\bar{\mathbf{x}} \in \mathcal{X}$) has been used as a standard stationarity measure in nonsmooth optimization (see, e.g., [17], [18], [24]), where $d(\cdot, \cdot)$ stands for the distance between a given point and a given subset in \mathcal{X} . Even for $\phi \neq 0$, $\mathcal{M}_{\gamma}^{f, \phi}$ works as a stationarity measure at $\bar{\mathbf{x}} \in \mathcal{X}$ for Problem I.1 because [19, p.243]

$$(\forall \gamma \in \mathbb{R}_{++}) \quad \partial f(\bar{\mathbf{x}}) + \partial\phi(\bar{\mathbf{x}}) \ni \mathbf{0} \Leftrightarrow \mathcal{M}_{\gamma}^{f, \phi}(\bar{\mathbf{x}}) = 0.$$

Thus, finding a stationary point $\mathbf{x}^* \in \mathcal{X}$ of Problem I.1 is equivalent to finding \mathbf{x}^* such that $\mathcal{M}_{\gamma}^{f, \phi}(\mathbf{x}^*) = 0$.

From a viewpoint of approximating a stationary point $\mathbf{x}^* \in \mathcal{X}$ with an iterative update of estimates $(\mathbf{x}_n)_{n=1}^{\infty} \subset \mathcal{X}$ of \mathbf{x}^* , a stationarity measure is desired to have a lower semicontinuous property^{b)}. Fortunately, $\mathcal{M}_{\gamma}^{f, \phi}$ in (5) of our interest is lower semicontinuous, and $\mathcal{M}_{\gamma}^{f, \phi}$ can be approximated with a smoothed surrogate function $h + \mu g \circ \mathfrak{S}$ of $f = h + g \circ \mathfrak{S}$.

Theorem III.1. Consider Problem I.1. For arbitrarily given $\bar{\mathbf{x}} \in \mathcal{X}$ and $(\mathbf{x}_n)_{n=1}^{\infty} \subset \mathcal{X}$ such that $\lim_{n \rightarrow \infty} \mathbf{x}_n = \bar{\mathbf{x}}$, the following hold:

(a) (Lower semicontinuity of $\mathcal{M}_{\gamma}^{f, \phi}$)

$$(\gamma \in \mathbb{R}_{++}) \quad \liminf_{n \rightarrow \infty} \mathcal{M}_{\gamma}^{f, \phi}(\mathbf{x}_n) \geq \mathcal{M}_{\gamma}^{f, \phi}(\bar{\mathbf{x}}),$$

where $\liminf_{n \rightarrow \infty}$ denotes the standard limit inferior for a real number sequence.

(b) (Smooth approximation of $\mathcal{M}_{\gamma}^{f, \phi}$) Let $(\mu_n)_{n=1}^{\infty} \subset (0, \eta^{-1})$ satisfy $\mu_n \searrow 0$ ($n \rightarrow \infty$), and $f_n := h + \mu_n g \circ \mathfrak{S}$. Then,

$$(\gamma \in \mathbb{R}_{++}) \quad \liminf_{n \rightarrow \infty} \mathcal{M}_{\gamma}^{f_n, \phi}(\mathbf{x}_n) \geq \mathcal{M}_{\gamma}^{f, \phi}(\bar{\mathbf{x}}).$$

Moreover, if $\liminf_{n \rightarrow \infty} \mathcal{M}_{\gamma}^{f_n, \phi}(\mathbf{x}_n) = 0$ with some $\gamma \in \mathbb{R}_{++}$, then $\bar{\mathbf{x}}$ is a stationary point of $f + \phi$.

Theorem III.1 (b) implies that our goal for finding a stationary point $\mathbf{x}^* \in \mathcal{X}$ of Problem I.1 is reduced to the following problem:

find a convergent $(\mathbf{x}_n)_{n=1}^{\infty} \subset \mathcal{X}$ such that $\liminf_{n \rightarrow \infty} \mathcal{M}_{\gamma}^{f_n, \phi}(\mathbf{x}_n) = 0$

with some $\gamma \in \mathbb{R}_{++}$ and $f_n := h + \mu_n g \circ \mathfrak{S}$ ($\mu_n \searrow 0$). In order to find such a sequence $(\mathbf{x}_n)_{n=1}^{\infty}$, we propose a proximal variable smoothing illustrated in Algorithm 1.

The proposed Algorithm 1 is designed as a time-varying forward-backward splitting-type algorithm. In the forward step at n th iteration, we perform a gradient descent at the latest estimate $\mathbf{x}_n \in \mathcal{X}$ as $\mathbf{x}_{n+\frac{1}{2}} := \mathbf{x}_n - \gamma_n \nabla f_n(\mathbf{x}_n) \in \mathcal{X}$ with a smoothed surrogate function f_n and a stepsize γ_n . In the backward step at n th iteration, we assign $\text{prox}_{\gamma_n \phi}(\mathbf{x}_{n+\frac{1}{2}})$ to the next estimate $\mathbf{x}_{n+1} \in \mathcal{X}$.

The index $\mu_n \in (0, 2^{-1}\eta^{-1})$ of $\mu_n g$ is designed to satisfy

$$\left\{ \begin{array}{l} \text{(i) } \lim_{n \rightarrow \infty} \mu_n = 0, \text{ (ii) } \sum_{n=1}^{\infty} \mu_n = +\infty, \\ \text{(iii) } (\exists M \geq 1, \forall n \in \mathbb{N}) \quad M^{-1} \leq \mu_{n+1}/\mu_n \leq 1. \end{array} \right. \quad (6)$$

^{b)}To explain this, let $\mathcal{M} : \mathcal{X} \rightarrow \mathbb{R}$ be a stationarity measure with lower semicontinuity. In this case, even if any cluster point of $(\mathbf{x}_n)_{n=1}^{\infty} \subset \mathcal{X}$ is not a stationary point, then $\liminf_{n \rightarrow \infty} \mathcal{M}(\mathbf{x}_n) = 0$ may hold [30, p. 837].

For example, $(\mu_n)_{n=1}^\infty := ((2\eta)^{-1}n^{-1/\alpha})_{n=1}^\infty$ with $\alpha \geq 1$ enjoys (6), and $\alpha = 3$ has been used as a standard choice of $(\mu_n)_{n=1}^\infty$ to achieve a reasonable convergence rate in variable smoothing [17], [19].

Every stepsize $\gamma_n \in \mathbb{R}_{++}$ in Algorithm 1 is chosen to satisfy an Armijo-type condition (see, e.g., [31]) with $\gamma := \gamma_n$ and $c \in (0, 1)$:

$$(f_n + \phi)(\text{prox}_{\gamma\phi}(\mathbf{x}_n - \gamma\nabla f_n(\mathbf{x}_n))) \leq (f_n + \phi)(\mathbf{x}_n) - c\gamma (\mathcal{M}_{\gamma}^{f_n, \phi}(\mathbf{x}_n))^2. \quad (7)$$

The existence of such a stepsize γ_n is guaranteed under the Lipschitz continuity of ∇f_n (see Assumption III.2 and Remark III.3).

Assumption III.2. Consider Problem I.1 and Algorithm 1. For $f_n = h + \mu_n g \circ \mathfrak{S}$, we assume:

- (a) (Gradient Lipschitz continuity condition) There exist $\varpi_1, \varpi_2 \in \mathbb{R}_{++}$ such that ∇f_n ($n \in \mathbb{N}$) is Lipschitz continuous with a Lipschitz constant $L_{\nabla f_n} := \varpi_1 + \varpi_2 \mu_n^{-1}$.
- (b) (Lower bound condition for stepsizes) For some $c \in (0, 1)$ and $\beta \in \mathbb{R}_{++}$, γ_n ($n \in \mathbb{N}$) satisfies (i) the Armijo-type condition (7) with $\gamma := \gamma_n$; (ii) $\gamma_n \geq \beta L_{\nabla f_n}^{-1}$; and (iii) $\bar{\gamma} := \sup_{n \in \mathbb{N}} \gamma_n < +\infty$.

Remark III.3 (Examples achieving Assumption III.2).

- (a) Assumption III.2 (a) is satisfied if (i) $\|\text{D}\mathfrak{S}(\cdot)\|_{\text{op}}$ is bounded over $\text{dom}(\phi)$ and (ii) $\text{D}\mathfrak{S}(\cdot)$ is Lipschitz continuous over $\text{dom}(\phi)$ [18]. Clearly, Assumption III.2 (a) is automatically satisfied if \mathfrak{S} is linear.
- (b) We have mainly two choices of γ_n enjoying Assumption III.2 (b) [31]. The first choice is $\gamma_n := 2(1-c)L_{\nabla f_n}^{-1}$. The second choice is given by the so-called *backtracking algorithm* (see, e.g., [31]), i.e., $\gamma_n := \max\{\gamma_{\text{initial}}\rho^k \mid k \in \mathbb{N} \cup \{0\}, \gamma := \gamma_{\text{initial}}\rho^k \text{ satisfies (7)}\}$ with $\gamma_{\text{initial}} \in \mathbb{R}_{++}$ and $\rho \in (0, 1)$. For the second choice, any knowledge on $L_{\nabla f_n}$ is not required.

We present below a convergence analysis of Algorithm 1.

Theorem III.4 (Convergence analysis of Alg. 1). Consider Problem I.1. Choose arbitrarily $\mathbf{x}_1 \in \text{dom}(\phi)$, $c \in (0, 1)$, and $(\mu_n)_{n=1}^\infty \subset (0, (2\eta)^{-1}]$ satisfying (6). Suppose that $(\mathbf{x}_n)_{n=1}^\infty \subset \mathcal{X}$ is generated by Alg. 1 under Assumption III.2. Then, the following hold:

- (a) With $\bar{\gamma} = \sup_{n \in \mathbb{N}} \gamma_n < +\infty$ in Assumption III.2 (b),

$$\liminf_{n \rightarrow \infty} \mathcal{M}_{\bar{\gamma}}^{f_n, \phi}(\mathbf{x}_n) = 0.$$

(Proof is partially inspired by [19, Lemma 9])

- (b) We can choose a subsequence $(\mathbf{x}_{m(l)})_{l=1}^\infty \subset \mathcal{X}$ of $(\mathbf{x}_n)_{n=1}^\infty$ such that $\lim_{l \rightarrow \infty} \mathcal{M}_{\bar{\gamma}}^{f_{m(l)}, \phi}(\mathbf{x}_{m(l)}) = 0$, where $m : \mathbb{N} \rightarrow \mathbb{N}$ is monotonically increasing. Moreover, every cluster point $\mathbf{x}^* \in \mathcal{X}$ of $(\mathbf{x}_{m(l)})_{l=1}^\infty$ is a stationary point of Problem I.1 (This statement can be checked by combining (a) with Theorem III.1 (b)).

Remark III.5 (Relation to previous works [17]–[19]).

- (a) (Variable smoothing in [17], [18]) For Problem I.1 with a special case $\phi := 0$, Algorithm 1 reproduces a variable smoothing in [17], [18]. Indeed, a stationarity measure used in [17], [18] can be expressed as $\mathcal{M}_{\gamma}^{f, \phi}$ with a special case $\phi = 0$.
- (b) (Proximal variable smoothing in [19]) For Problem I.1 with a special case where \mathfrak{S} is surjective and linear, Algorithm 1 reproduces a proximal variable smoothing in [19, Alg. 1]. A convergence analysis in [19, Theorem 1] of [19, Alg. 1] provides only a bound of the number of iterations to achieve $\mathcal{M}_{\gamma}^{f, \phi}(\mathbf{x}_n) < \epsilon$ for a given $\epsilon \in \mathbb{R}_{++}$. In contrast, thanks to Theorem III.1, Theorem III.4 ensures an asymptotic convergence of Alg. 1 in more general settings than the surjective and linearity of \mathfrak{S} assumed in [19] (Note: Assumption III.2 (a) is automatically satisfied if \mathfrak{S} is linear [see Remark III.3 (a)]).

IV. APPLICATION TO MU-MIMO SIGNAL DETECTION

A. Formulation of MU-MIMO Signal Detection via Problem I.1

To evaluate the performance of Algorithm 1, we carried out numerical experiments in a scenario of massive multiuser multiple-input-multiple-output (MU-MIMO) signal detection using M ($\in \mathbb{N}$)-ary phase-shift keying (see, e.g., [20]–[23]). This task is reduced to

$$\text{find } \mathbf{s}^* \in \mathcal{D} \subset \mathbb{C}^U \text{ from } \mathbf{y} = \mathbf{H}\mathbf{s}^* + \mathbf{e} \in \mathbb{C}^B, \quad (8)$$

where $\mathbf{s}^* \in \mathcal{D} := \{\exp(i2\pi m/M) \in \mathbb{C} \mid m = 0, 1, \dots, M-1\}^U \subset \mathbb{C}^U$ is the transmit vector, $\mathbf{y} \in \mathbb{C}^B$ is the received vector with a known measurement matrix $\mathbf{H} \in \mathbb{C}^{B \times U}$, $\mathbf{e} \in \mathbb{C}^B$ is noise, \mathcal{D} is a discrete set called a *constellation set*, and $U, B \in \mathbb{N}$ ($U > B$) are respectively the numbers of transmitting and receiving antennas. The task (8) with the case $U > B$ has appeared in, e.g., typical IoT environments [21].

Usually, MU-MIMO signal detection problem in (8) has been tackled via real-valued optimization problems [20], [21], [23] as

$$\underset{\mathbf{s} \in \mathcal{C} \subset \mathbb{R}^{2U}}{\text{minimize}} \quad \frac{1}{2} \|\mathbf{y} - \mathbf{H}\mathbf{s}\|^2 + \lambda\psi(\mathbf{s}) \quad (9)$$

with the real-valued expressions of \mathbf{y} and \mathbf{H} :

$$\mathbf{y} := \hat{\mathbf{y}} := \begin{bmatrix} \Re(\mathbf{y}) \\ \Im(\mathbf{y}) \end{bmatrix} \in \mathbb{R}^{2B}, \quad \mathbf{H} := \begin{bmatrix} \Re(\mathbf{H}) & -\Im(\mathbf{H}) \\ \Im(\mathbf{H}) & \Re(\mathbf{H}) \end{bmatrix} \in \mathbb{R}^{2B \times 2U}, \quad (10)$$

where a constraint set $(\emptyset \neq) \mathcal{C} \subset \mathbb{R}^{2U}$ is designed to contain the real-valued expression $\mathfrak{D} := \{\hat{\mathbf{s}} \mid \mathbf{s} \in \mathcal{D}\} \subset \mathbb{R}^{2U}$ of \mathcal{D} , $\lambda \in \mathbb{R}_{++}$ is a weight and $\psi : \mathbb{R}^{2U} \rightarrow \mathbb{R}$ is a regularizer. For example, a classical linear minimum mean-square-error detection (denoted by ‘‘LMMSE’’), e.g., [20], considers the problem (9) with $\psi := \|\cdot\|^2$ and $\mathcal{C} := \mathbb{R}^{2U}$, where $\lambda := \sigma^2/2$ is given by the variance σ^2 of \mathbf{e} in (8). In this case, the closed-form solution is given by $(\mathbf{H}^\top \mathbf{H} + \sigma^2 \mathbf{I})^{-1} \mathbf{H}^\top \mathbf{y}$. The reference [21] proposed a modulus-constrained least squares model (9) (denoted by ‘‘Modulus’’) where $\psi := 0$, and $\mathcal{C} := \{\hat{\mathbf{z}} \mid \mathbf{z} \in \mathbb{T}^U\} \subset \mathbb{R}^{2U}$ with $\mathbb{T} := \{z \in \mathbb{C} \mid |z| = 1\}$ (Note: the modulus constraint \mathcal{C} is designed as a superset of \mathfrak{D}). Moreover, [23] proposed the so-called SOAV model (9) (denoted by ‘‘SOAV’’) where \mathcal{C} is the convex hull of \mathfrak{D} and ψ is the *sum-of-absolute-value (SOAV)* function [32]. The SOAV function $\psi_{\text{SOAV}} := \frac{1}{M} \sum_{m=1}^M \|\cdot - \hat{\mathbf{s}}_m\|_1$ is designed to penalize a given $\mathbf{s} \in \mathbb{R}^{2U}$ that deviates from discrete-valued points in \mathfrak{D} , where $\mathbf{s}_m := \exp(i2\pi m/M) \mathbf{1} \in \mathcal{D}$ and $\hat{\mathbf{s}}_m \in \mathfrak{D}$ ($m = 0, 1, \dots, M-1$) (see (10) for (\cdot)). However, the penalization by ψ_{SOAV} is not contrastive enough to distinguish between points in \mathfrak{D} and the other points because any point in \mathfrak{D} is never unique minimizer of ψ_{SOAV} due to its convexity^o.

In this paper, for (8), we propose a new model with a more contrastive regularizer $\psi_{\lambda_r, \lambda_\theta}$ than the SOAV function ψ_{SOAV} as:

$$\underset{\substack{\mathbf{r} \in [r_{\min}, 1], \\ \boldsymbol{\theta} \in \mathbb{R}^U}}{\text{minimize}} \quad \frac{1}{2} \|\mathbf{y} - \mathbf{H}\mathbf{F}(\mathbf{r}, \boldsymbol{\theta})\|^2 + \lambda_r \underbrace{\sum_{u=1}^U [\mathbf{r}]_u^{-1} + \lambda_\theta \left\| \sin\left(\frac{\mathbf{M}\boldsymbol{\theta}}{2}\right) \right\|_1}_{=: \psi_{\lambda_r, \lambda_\theta}(\mathbf{r}, \boldsymbol{\theta})}, \quad (11)$$

where we use a polar coordinate-type expression of \mathbf{s} in (9) as:

$$\mathbf{F} : \mathbb{R}^U \times \mathbb{R}^U \rightarrow \mathbb{R}^{2U} : (\mathbf{r}, \boldsymbol{\theta}) \mapsto \mathbf{s} := \begin{bmatrix} \mathbf{r} \odot \sin(\boldsymbol{\theta}) \\ \mathbf{r} \odot \cos(\boldsymbol{\theta}) \end{bmatrix},$$

i.e., $\mathbf{r}, \boldsymbol{\theta}$ denote respectively the radial and angle coordinates of \mathbf{s} , $\sin : \mathbb{R}^U \times \mathbb{R}^U \rightarrow \mathbb{R}^U : \boldsymbol{\theta} \mapsto [\sin([\boldsymbol{\theta}]_1) \ \sin([\boldsymbol{\theta}]_2) \ \dots \ \sin([\boldsymbol{\theta}]_U)]^\top$

^oAs more contrastive regularizers than the SOAV function ψ_{SOAV} , non-convex regularizers $\psi := \frac{1}{M} \sum_{m=1}^M \|\cdot - \hat{\mathbf{s}}_m\|_p$ have been proposed [22] with ℓ_p -pseudonorm $\|\cdot\|_p$ ($p \in [0, 1)$). However, for the problem (9) with this nonconvex ψ , any solver guaranteed with convergence has not been found yet as remarked in [22] due to the severe nonconvexity.

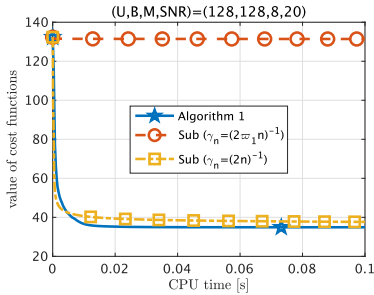


Fig. 1. Convergence history

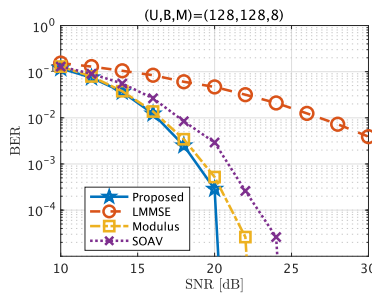


Fig. 2. BER vs SNR ($B = U$)

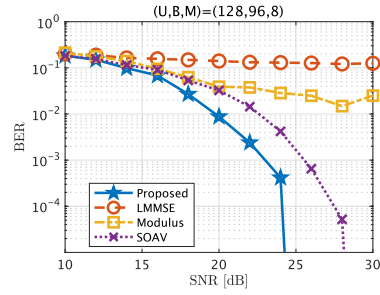


Fig. 3. BER vs SNR ($B = \frac{3}{4}U$)

(so as \cos), $r_{\min} \in (0, 1]$ is the smallest value for each $[\mathbf{r}]_u$, and $\lambda_r, \lambda_\theta \in \mathbb{R}_{++}$ are weights.

The proposed $\psi_{\lambda_r, \lambda_\theta}$ in (11) penalizes (i) small radius $[\mathbf{r}]_u$ and (ii) angle $[\boldsymbol{\theta}]_u$ that deviates from desired angles $\{2\pi m/M \mid m \in \mathbb{Z}\}$ (see D just after (8)). Indeed, for any $\lambda_r, \lambda_\theta \in \mathbb{R}_{++}$, we can check:

$$F(\mathbf{r}^*, \boldsymbol{\theta}^*) \in \mathcal{D} \Leftrightarrow (\mathbf{r}^*, \boldsymbol{\theta}^*) \in \underset{(\mathbf{r}, \boldsymbol{\theta}) \in [r_{\min}, 1]^U \times \mathbb{R}^U}{\operatorname{argmin}} \psi_{\lambda_r, \lambda_\theta}(\mathbf{r}, \boldsymbol{\theta}) \\ (= \{(\mathbf{1}, 2\pi \mathbf{m}/M) \mid \mathbf{m} \in \mathbb{Z}^U\}), \quad (12)$$

implying thus $\psi_{\lambda_r, \lambda_\theta}$ is a desired regularizer to penalize a point $\mathbf{s} = F(\mathbf{r}, \boldsymbol{\theta})$ that deviates from points in \mathcal{D} . To examine a potential of the basic idea^{d)} in $\psi_{\lambda_r, \lambda_\theta}$, we will present the numerical performance of the model (11), which can be formulated as Problem I.1^{e)} with $\mathcal{X} := \mathbb{R}^U \times \mathbb{R}^U$, $\mathcal{Z} := \mathbb{R}^U$, and

$$h: \mathcal{X} \rightarrow \mathbb{R}: (\mathbf{r}, \boldsymbol{\theta}) \mapsto \frac{1}{2} \|\mathbf{y} - \mathbf{H}F(\mathbf{r}, \boldsymbol{\theta})\|^2 + \lambda_r \sum_{u=1}^U [\mathbf{r}]_u^{-1}, \\ \mathfrak{S}: \mathcal{X} \rightarrow \mathcal{Z}: (\mathbf{r}, \boldsymbol{\theta}) \mapsto \sin\left(\frac{M\boldsymbol{\theta}}{2}\right), \quad g: \mathcal{Z} \rightarrow \mathbb{R}: \mathbf{z} \mapsto \lambda_\theta \|\mathbf{z}\|_1, \\ \phi: \mathcal{X} \rightarrow \mathbb{R} \cup \{+\infty\}: (\mathbf{r}, \boldsymbol{\theta}) \mapsto \begin{cases} 0, & \text{if } (\mathbf{r}, \boldsymbol{\theta}) \in [r_{\min}, 1]^U \times \mathbb{R}^U; \\ +\infty, & \text{if } (\mathbf{r}, \boldsymbol{\theta}) \notin [r_{\min}, 1]^U \times \mathbb{R}^U. \end{cases}$$

Assumption III.2 (a) holds with, e.g., $\varpi_1 := 4((2 + \sqrt{U}) \|\mathbf{H}\|_{\text{op}}^2 + \|\mathbf{H}^T \mathbf{y}\|) + 2\sqrt{U} \lambda_r r_{\min}^{-4} + 2^{-1} \sqrt{U} \lambda_\theta M$ and $\varpi_2 := 4^{-1} M^2$, and thus a stationary point of (11) can be obtained by Alg. 1 (see Thm. III.4)

B. Numerical Experiments

We evaluated numerical performance of the proposed model (11) and Alg. 1 under the setting^{f)} in [21]. For Alg. 1, we employed $(\mu_n)_{n=1}^\infty := ((2\eta)^{-1} n^{-1/3})_{n=1}^\infty$, $c = 2^{-13}$, $\eta = 1$, and $(\gamma_n)_{n=1}^\infty$ given by the backtracking algorithm (see Remark III.3 (b)) with $\gamma_{\text{initial}} := 1$ and $\rho := 2^{-1}$. All experiments were performed by MATLAB on MacBookPro (Apple M3, 16 GB).

We firstly compared convergence performance of Alg. 1 with that of a fairly standard nonsmooth optimization algorithm, called proximal subgradient method (denoted by “Sub”) [33], in a scenario of the problem (11). “Sub” in [33] updates $\mathbf{x}_{n+1} := \operatorname{prox}_{\gamma_n \phi}(\mathbf{x}_n - \gamma_n \mathbf{v}_n) \in \mathcal{X}$ at n th iteration with $\mathbf{x}_n \in \mathcal{X}$, $\mathbf{v}_n \in \partial(h + g \circ \mathfrak{S})(\mathbf{x}_n)$ and $\gamma_n \in \mathbb{R}_{++}$. For “Sub”, we employed two stepsizes: (i) $\gamma_n := (2\varpi_1 n)^{-1}$, with ϖ_1 given in Sect. IV-A, which guarantees a convergence to a

^{d)}The desired property (12) holds even if $\|\cdot\|_1$ in $\psi_{\lambda_r, \lambda_\theta}$ is replaced by weakly convex functions, e.g., MCP [2], and SCAD [3].

^{e)} g and ϕ are prox-friendly (see, e.g., [1, Exm. 24.20] and [31, Lem. 6.26]).

^{f)}For the problem (8), we randomly chose (i) $\mathbf{s}^* \in \mathcal{D}$; (ii) $\mathbf{H} := \sqrt{R}\mathbf{G}$ with $\mathbf{G} \in \mathbb{C}^{B \times U}$ whose entries were sampled from the complex Gaussian distribution $\mathcal{CN}(0, 1/U)$, and a symmetric Toeplitz matrix $\mathbf{R} \in \mathbb{R}^{B \times B}$ whose entries were given by $[\mathbf{R}]_{j,k} = 0.5|j-k|$; and (iii) $\mathbf{e} \in \mathbb{C}^B$ whose entries were sampled from $\mathcal{CN}(0, \sigma^2)$, where σ^2 was chosen so that $10 \log_{10} \frac{1}{\sigma^2}$ (dB) achieved a given signal-to-noise ratio (SNR).

stationary point [33, Lem. 4.3 and Thm. 4.1]; and (ii) heuristic $\gamma_n := (2n)^{-1g}$. We employed parameters in (11) as $\lambda_r = \lambda_\theta = r_{\min} = 0.1$ under $(U, B, M, \text{SNR}) = (128, 128, 8, 20)$ (dB). All algorithms were terminated when running CPU time exceeded 0.1 (s).

Fig. 1 shows the averaged values of the cost function over 100 trials versus CPU time (s) for Alg. 1 and “Sub”, where markers were put at every 100 iterations. From Fig. 1, we observe that Alg. 1 converges much faster than “Sub” with stepsize $\gamma_n = (2\varpi_1 n)^{-1}$ with guaranteed convergence. Moreover, Alg. 1 also achieves faster convergence speed than “Sub” with heuristic stepsize $\gamma_n = (2n)^{-1}$. This result implies an effective convergence performance of Alg. 1.

Next, we compared estimation performance of (i) the proposed model (11)^{h)}, solved by Alg. 1, with that of three models: (ii) “LMMSE”, e.g., [20], (iii) “Modulus”ⁱ⁾ [21], and (iv) “SOAV”^{j)} [23] (see just after (9) for (ii)-(iv) in detail). All algorithms except “LMMSE” were terminated when running CPU time exceeded 3 (s) or $\|\mathbf{x}_{n+1} - \mathbf{x}_n\| \leq 10^{-5}$ held with a sequence $(\mathbf{x}_n)_{n=1}^\infty$ generated by algorithms. As a performance criterion, we employed averaged bit error rate (BER)^{k)} of the final estimate over 100 trials. The lower averaged BER indicates better estimate performance.

Figs. 2 and 3 demonstrate the averaged BER of each algorithm versus SNR under respectively two settings $B = U$ and $B = \frac{3}{4}U$, where the averaged BER 0 was replaced by the machine epsilon. We note that the estimation task (8) becomes challenging as the ratio B/U becomes small. From Figs. 2 and 3, we observe that (i) every model achieves better performance than “LMMSE”; (ii) the proposed model in (11) outperforms the others for all SNRs and ratios B/U . In particular, from Fig. 3, we see that the proposed model in (11) overwhelms the others in the challenging setting with $B = \frac{3}{4}U$. As we expected, these results show a great potential of the proposed model in (11) and Alg. 1 for MU-MIMO signal detection.

V. CONCLUSION

We proposed a proximal variable smoothing for nonsmooth minimization involving weakly convex composite in Problem I.1. The proposed algorithm consists of two steps: (i) a time-varying forward step with the gradient of a smoothed surrogate function designed with the Moreau envelope; (ii) the backward step with the proximity operator. We also presented an asymptotic convergence analysis of the proposed algorithm. Numerical experiments in a scenario of MU-MIMO demonstrate the effectiveness of (i) the proposed algorithm and (ii) a new formulation in (11) of MU-MIMO by Problem I.1.

^{g)}Although the difference between two stepsizes is only a constant factor, convergence is not guaranteed for “Sub” with the latter heuristic stepsize.

^{h)} $\lambda_r, \lambda_\theta$ were chosen from $\{10^k \mid k = -6, -5, \dots, 0\}$ and $r_{\min} = 0.1$.

ⁱ⁾We applied a projected gradient method [21] to “Modulus”.

^{j)} λ in (9) was chosen from $\{10^k \mid k = -6, -5, \dots, 1\}$. We applied a primal-dual splitting algorithm [34] to “SOAV”.

^{k)}BER was computed by a MATLAB code with ‘pskdemod’ and ‘biterr’.

REFERENCES

- [1] H. H. Bauschke and P. L. Combettes, *Convex analysis and monotone operator theory in Hilbert spaces*, 2nd ed. Springer, 2017.
- [2] C.-H. Zhang, “Nearly unbiased variable selection under minimax concave penalty,” *The Annals of Statistics*, vol. 38, no. 2, pp. 894–942, 2010.
- [3] J. Fan and R. Li, “Variable selection via nonconcave penalized likelihood and its oracle properties,” *Journal of the American Statistical Association*, vol. 96, no. 456, pp. 1348–1360, 2001.
- [4] J. Li, A. M. C. So, and W. K. Ma, “Understanding notions of stationarity in nonsmooth optimization: A guided tour of various constructions of subdifferential for nonsmooth functions,” *IEEE Signal Processing Magazine*, vol. 37, no. 5, pp. 18–31, 2020.
- [5] S. Gandy, B. Recht, and I. Yamada, “Tensor completion and low-n-rank tensor recovery via convex optimization,” *Inverse Problems*, vol. 27, no. 2, p. 025010, 2011.
- [6] L. Yin, A. Parekh, and I. Selesnick, “Stable principal component pursuit via convex analysis,” *IEEE Transactions on Signal Processing*, vol. 67, no. 10, pp. 2595–2607, 2019.
- [7] H. Kuroda and D. Kitahara, “Block-sparse recovery with optimal block partition,” *IEEE Transactions on Signal Processing*, vol. 70, pp. 1506–1520, 2022.
- [8] P. L. Combettes and J.-C. Pesquet, “Fixed point strategies in data science,” *IEEE Transactions on Signal Processing*, vol. 69, pp. 3878–3905, 2021.
- [9] Z. Zheng, S. Ma, and L. Xue, “A new inexact proximal linear algorithm with adaptive stopping criteria for robust phase retrieval,” *IEEE Transactions on Signal Processing*, vol. 72, pp. 1081–1093, 2024.
- [10] Z.-Y. Wang, H. C. So, and A. M. Zoubir, “Robust low-rank matrix recovery via hybrid ordinary-Welsch function,” *IEEE Transactions on Signal Processing*, vol. 71, pp. 2548–2563, 2023.
- [11] V. Charisopoulos, D. Davis, M. Díaz, and D. Drusvyatskiy, “Composite optimization for robust rank one bilinear sensing,” *Information and Inference: A Journal of the IMA*, vol. 10, no. 2, pp. 333–396, 2020.
- [12] A. S. Lewis and S. J. Wright, “A proximal method for composite minimization,” *Mathematical Programming*, vol. 158, no. 1, pp. 501–546, 2016.
- [13] D. Drusvyatskiy and C. Paquette, “Efficiency of minimizing compositions of convex functions and smooth maps,” *Mathematical Programming*, vol. 178, no. 1, pp. 503–558, 2019.
- [14] D. Davis and W. Yin, “A Three-Operator Splitting Scheme and its Optimization Applications,” *Set-Valued and Variational Analysis*, vol. 25, no. 4, pp. 829–858, 2017.
- [15] R. Zhao and V. Cevher, “Stochastic three-composite convex minimization with a linear operator,” in *AISTATS*, vol. 84, 2018, pp. 765–774.
- [16] L. Condat, D. Kitahara, A. Contreras, and A. Hirabayashi, “Proximal splitting algorithms for convex optimization: a tour of recent advances, with new twists,” *SIAM Review*, vol. 65, no. 2, pp. 375–435, 2023.
- [17] A. Böhm and S. J. Wright, “Variable smoothing for weakly convex composite functions,” *Journal of Optimization Theory and Applications*, vol. 188, no. 3, pp. 628–649, 2021.
- [18] K. Kume and I. Yamada, “A variable smoothing for nonconvexly constrained nonsmooth optimization with application to sparse spectral clustering,” in *IEEE ICASSP*, 2024, pp. 9296–9300.
- [19] Y. Liu and F. Xia, “Proximal variable smoothing method for three-composite nonconvex nonsmooth minimization with a linear operator,” *Numerical Algorithms*, vol. 96, no. 1, pp. 237–266, 2024.
- [20] S. Yang and L. Hanzo, “Fifty years of MIMO detection: The road to large-scale MIMOs,” *IEEE Communications Surveys & Tutorials*, vol. 17, no. 4, pp. 1941–1988, 2015.
- [21] J. C. Chen, “Computationally efficient data detection algorithm for massive MU-MIMO systems using PSK modulations,” *IEEE Communications Letters*, vol. 23, no. 6, pp. 983–986, 2019.
- [22] R. Hayakawa and K. Hayashi, “Discrete-valued vector reconstruction by optimization with sum of sparse regularizers,” in *EUSIPCO*. EURASIP, 2019, pp. 1–5.
- [23] —, “Asymptotic performance of discrete-valued vector reconstruction via box-constrained optimization with sum of ℓ_1 regularizers,” *IEEE Transactions on Signal Processing*, vol. 68, pp. 4320–4335, 2020.
- [24] R. Rockafellar and R. J.-B. Wets, *Variational Analysis*, 3rd ed. Springer Verlag, 2010.
- [25] I. Yamada, M. Yukawa, and M. Yamagishi, “Minimizing the Moreau envelope of nonsmooth convex functions over the fixed point set of certain quasi-nonexpansive mappings,” in *Fixed-Point Algorithms for Inverse Problems in Science and Engineering*, H. H. Bauschke, R. S. Burachik, P. L. Combettes, V. Elser, D. R. Luke, and H. Wolkowicz, Eds. Springer New York, 2011, pp. 345–390.
- [26] J. Abe, M. Yamagishi, and I. Yamada, “Linearly involved generalized Moreau enhanced models and their proximal splitting algorithm under overall convexity condition,” *Inverse Problems*, vol. 36, no. 3, 2020.
- [27] H. H. Bauschke, W. M. Moursi, and X. Wang, “Generalized monotone operators and their averaged resolvents,” *Mathematical Programming*, vol. 189, no. 1, pp. 55–74, 2021.
- [28] G. Chierchia, E. Chouzenoux, P. L. Combettes, and J.-C. Pesquet, “The proximity operator repository.” [Online]. Available: <http://proximity-operator.net/>
- [29] T. Hoheisel, M. Laborde, and A. Oberman, “A regularization interpretation of the proximal point method for weakly convex functions,” *Journal of Dynamics and Games*, vol. 7, no. 1, pp. 79–96, 2020.
- [30] E. Levin, J. Kileel, and N. Boumal, “Finding stationary points on bounded-rank matrices: a geometric hurdle and a smooth remedy,” *Mathematical Programming*, vol. 199, no. 1, pp. 831–864, 2023.
- [31] A. Beck, *First-Order Methods in Optimization*. SIAM, 2017.
- [32] M. Nagahara, “Discrete signal reconstruction by sum of absolute values,” *IEEE Signal Processing Letters*, vol. 22, no. 10, pp. 1575–1579, 2015.
- [33] D. Zhu, L. Zhao, and S. Zhang, “A unified analysis for the subgradient methods minimizing composite nonconvex, nonsmooth and non-Lipschitz functions,” *arXiv (2308.16362)*, pp. 1–32, 2023.
- [34] L. Condat, “A primal–dual splitting method for convex optimization involving Lipschitzian, proximable and linear composite terms,” *Journal of Optimization Theory and Applications*, vol. 158, no. 2, pp. 460–479, 2013.